ACCOUNTS of chemical research

Article

pubs.acs.org/accounts

Surfaces of Complex Intermetallic Compounds: Insights from Density Functional Calculations

Jürgen Hafner*,† and Marian Krajčí‡

†Faculty for Physics, Center for Computational Materials Science, Vienna University, Vienna, A-1090, Austria

‡Institute of Physics, Slovak Academy of Sciences, Bratislava, SK-84511, Slovakia

CONSPECTUS: Complex intermetallic compounds are a class of ordered alloys consisting of quasicrystals and other ordered compounds with large unit cells; many of them are approximant phases to quasicrystals. Quasicrystals are the limiting case where the unit cell becomes infinitely large; approximants are series of periodic structures converging to the quasicrystal. While the unique properties of quasicrystals have inspired many investigations of their surfaces, relatively little attention has been devoted to the surface properties of the approximants.

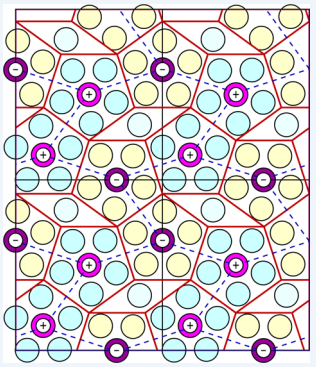

In general, complex intermetallic compounds display rather irregular, often strongly corrugated surfaces, making the determination of their atomic structure a very complex and challenging task. During recent years, scanning tunneling microscopy (STM) has been used to study the surfaces of several complex intermetallic compounds. If atomic resolution can be achieved, STM permits visualization of the local atomistic surface structure. However, the interpretation of the STM images is often ambiguous and sometimes even impossible without a realistic model of the structure of the surface and the distribution of the electronic density above the surface.

Here we demonstrate that *ab initio* density functional theory (DFT) can be used to determine the energetics and the geometric and electronic structures of the stable surfaces of complex intermetallic compounds. Calculations for surfaces with different chemical compositions can be performed in the grand canonical ensemble. Simulated cleavage experiments permit us to determine the formation of the cleavage planes requiring the lowest energy. The investigation of the adsorption of molecular species permits a comparison with temperature-programmed thermal desorption experiments. Calculated surface electronic densities of state can be compared with the results of photoelectron spectroscopy. Simulations of detailed STM images can be directly confronted with the experimental results.

Detailed results are presented for two intermetallic compounds that have recently attracted much attention as active and highly selective catalysts for the semihydrogenation of alkynes to alkenes, but the identification of the catalytically active surfaces was found to be very difficult. The crystal structure of B20-type GaPd can be interpreted as the lowest order approximant of icosahedral Al−Pd−Mn quasicrystals. Among the low-index surfaces, the {100} surface shows 2-fold symmetry and the {210} surface pseudo-5-fold symmetry; for both the surface stoichiometry is identical to that of the bulk. Because the structure lacks inversion symmetry, the {111} surfaces have polar character and permit terminations of widely different chemical composition. Results for all three surfaces are presented and compared with the available experiments. The crystal structure of orthorhombic $Al_{13}Co_4$ is built by pentagonal clusters similar to those found in decagonal Al−Co and Al−Ni−Co quasicrystals. A simulated cleavage experiment shows that the constituent clusters remain intact upon cleavage, resulting in the formation of a highly corrugated (100) surface. The calculated STM images are found to be in very good agreement with experiment and permit in addition identification of possible surface modifications by the desorption of individual atoms. Pentagonal motifs on the {210} surface of GaPd and on the (100) surface of $Al_{13}Co_4$ consisting of simple- and transition-metal atoms have been identified as the catalytically active centers for the semihydrogenation of acetylene to ethylene.

INTRODUCTION

While the low-index surfaces of pure metals have been studied for decades and are today well understood,[1,2] the investigations of the surfaces of intermetallic compounds have received much less attention. Complex intermetallic compounds are a class of ordered alloys consisting of quasicrystals and other ordered compounds with large unit cells; many of them are approximant phases to quasicrystals.[3] Their structure can often be described in terms of symmetric clusters decorating a large unit cell. Quasicrystals[4] are the limiting case where the unit cell becomes infinitely large. Approximants are series of periodic structures with a local order identical or at least similar to that in the quasicrystal, converging to the quasicrystal in the limit of an infinitely large unit cell. The unique structural properties of quasicrystals have also inspired a number of theoretical and experimental investigations of their surfaces.[5,6]

Because complex intermetallic compounds generally exhibit rather irregular, often strongly corrugated surfaces, the determination of their atomistic structure is a challenging task. A standard method for investigating the local structural

Special Issue: DFT Elucidation of Materials Properties

Received: February 3, 2014
Published: April 17, 2014

   dx.doi.org/10.1021/ar500043z | Acc. Chem. Res. 2014, 47, 3378−3384

order on surfaces is scanning tunneling microscopy (STM). At lower resolution, STM investigations show a sequence of smaller or larger flat terraces with step heights corresponding to the distance between the preferred cleavage planes. High-resolution STM images of individual terraces provide important information about the structure of the surface on a subnanometer scale and atomic resolution in the ideal case. However, from the STM images alone, it is extremely difficult to identify the observed terraces with possible cleavage planes. For understanding of the atomic surface structure, it is very helpful to compare experimental STM images with simulated STM images calculated using *ab initio* density-functional theory (DFT) for tentative structural models of the surface.

Using a combination of STM experiments and DFT calculations, the 5-fold surface of icosahedral Al−Pd−Mn quasicrystals[7−9] and the 10-fold surface of decagonal Al−Co−Ni quasicrystals[10,11] have been studied most intensively. It is surprising that despite their complex aperiodic structure, the surfaces can be atomically flat, such that high-resolution STM images with nearly atomic resolution can be achieved. Compared with the widespread interest in quasicrystalline surfaces, relatively little effort has been spent on the investigation of the surfaces of complex intermetallic compounds. Recently, the renewed interest in this subject has been triggered by the discovery that the surfaces of binary Pd−Ga[12,13] and Co(Fe)−Al[14,15] compounds are highly active and selective catalysts for the semihydrogenation of acetylene to ethylene. Some of the catalytically active compounds can be considered as approximants to icosahedral or decagonal quasicrystals.

In this Account, we discuss our current understanding of the surface structure of intermetallic compounds whose structure is closely related to quasicrystals, achieved by first-principles DFT calculations, and the confrontation of the results with STM images. DFT calculations with a gradient-corrected (GGA) exchange-correlation functional have been performed using the VASP program package,[16,17] which permits a full structural optimization of even very large structural models of surfaces. Surface energies have been calculated for sufficiently thick slab models using the grand-canonical formalism to determine the energies of surfaces with a stoichiometry differing from the bulk as a function of the chemical potential in the reactive atmosphere above the surface.[18,19] Simulated STM images have been calculated in the Tersoff−Hamann approximation.[20] For all further details, we refer to the original papers.[16−20]

■ B20-TYPE GA(AL)PD COMPOUNDS

GaPd and AlPd are isostructural intermetallic compounds crystallizing in the B20 structure. The B20 (FeSi-type) structure of Ga(Al)Pd with space group symmetry $P2_13$ exists in two enantiomorphic forms (labeled A and B) related by inversion.[21] The structure can be interpreted as a tiling of three-dimensional space with prolate and oblate rhombohedra, with Ga(Al) and Pd occupying opposite corners of each tile. Each atom is surrounded by seven atoms of the opposite kind forming an irregular polyhedron (see Figure 1). Along the 3-fold symmetry axis covalently bonded zigzag chains with alternating Ga(Al) and Pd atoms are found. The structure may be considered as the lowest-order approximant of icosahedral Al−Mn−Pd quasicrystals[8,22] whose electronic properties are also dominated by the bonding in similar Al−Pd chains.

Along the 2-fold {100} and the pseudo-5-fold {210} directions, the structure is built by a sequence of identical,

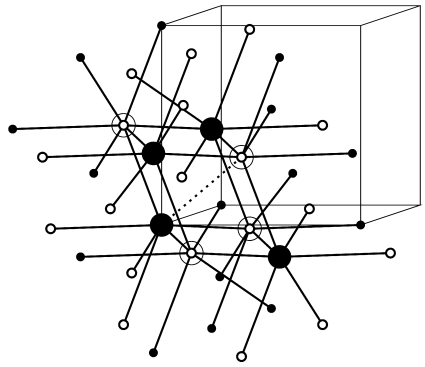

Figure 1. The B20 structure as a decorated tiling of prolate and oblate rhombohedra. One oblate rhombohedron is shown explicitly with the different atomic species decorating the vertices shown by the large full and empty circles. Each atom is coordinated by seven atoms of the opposite kind marked by smaller circles. See text.

slightly corrugated layers with the same stoichiometry as the bulk [see Figure 2a]. The surfaces normal to the 3-fold axes along the body diagonals of the unit cell have polar character. The A{111} surface is identical to the B{$\overline{1}\overline{1}\overline{1}$} surface and vice versa. Within a period along one of the 3-fold directions, there are nine atomic planes [see Figure 2]: three flat planes occupied by Pd only (marked P), three flat planes occupied by Ga only (G), and three slightly puckered planes with fixed Ga−Pd occupancy (M). Three consequent planes (P, M, and G) form a triplet stacked along a chiral screw axis, each following equivalent plane, for example, P, is rotated by $2\pi/3$ with respect to the previous P plane.[24]

The surface energies of the 2-fold {100} and of the pseudo-5-fold {210} surfaces can easily be calculated using standard slab techniques. For GaPd, their energies (γ_{100} = 1.01 J/m^2, γ_{210} = 1.08 J/m^2) are found to be equal to the average of the energies of the {100} surfaces of Ga (calculated for the *oP*8 structure) and face-centered cubic Pd (a similar relation holds for AlPd).[23−27] A relaxation of the surfaces shows that the interlayer distances change appreciably, but no surface reconstruction is observed. The atomic arrangement in the {210} plane shown in Figure 3 shows pseudo-5-fold symmetry, the atomic ordering may be described in terms of various tiling models: a hexagon−rhombus tiling (with acute angles of $2\pi/5$ emphasizing the pseudo-5-fold symmetry), a Penrose tiling obtained by splitting each hexagon into three thin rhombi (emphasizing the relation to the icosahedral structure of quasicrystals), and finally a triangle−rectangle (RT) tiling. The RT tiling is most helpful for understanding the chemical properties of the {210} surface of GaPd. The catalytically most active sites for the semihydrogenation of acetylene to ethylene are triangular arrangements of two Ga and one Pd atom. It has been shown that the key to the understanding of the exceptional selectivity of the GaPd catalyst is the change of the adsorption configuration, from acetylene strongly di-σ bound to a Ga−Ga bridge to ethylene weakly π-bonded on-top of the Pd atom.[23]

The {111} surfaces of GaPd have polar character; because of the sparse occupation each surface consists of a bilayer of two atomic planes. There are three bulk-terminated surfaces along the A[111] direction, PM, MG, and GP, and three, GM, MP, and PG, facing the A[$\overline{1}\overline{1}\overline{1}$] direction of the A form. Further surface terminations might be generated by splitting the puckered M layer into two very sparse planes denoted by g and p and occupied by only one atom per surface cell, M = g + p. This would require to distinguish four more possible surface

dx.doi.org/10.1021/ar500043z | Acc. Chem. Res. 2014, 47, 3378−3384

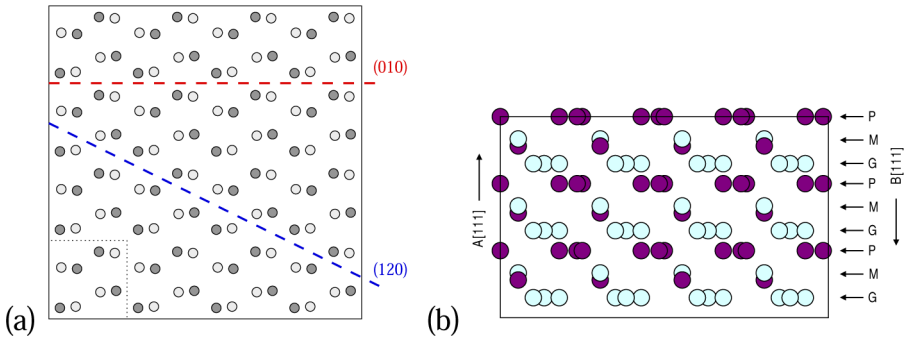

Figure 2. (a) The crystal structure of the A-form of B20-type GaPd projected onto the (001) plane, showing the cleavage planes determining the 2-fold (010) and the pseudo-5-fold (120) surfaces. (b) The layered structure along the polar [111] direction. In one period perpendicular to [111], there are nine atomic layers: three flat planes occupied by Pd only (P), three flat Ga layers (G), and three layers with mixed Ga–Pd occupancy (M). Atoms are shown by circles: Ga, light blue or light gray; Pd, violet or dark gray. See text.

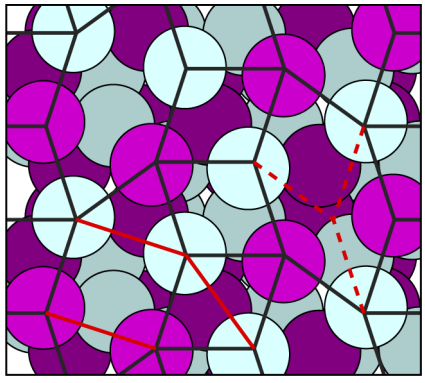

Figure 3. Top view of the pseudo-5-fold {210} surface of GaPd. A surface area of 2 unit cells is shown. Positions of atoms are shown by circles: Ga, light blue; Pd, magenta. The atoms below the top surface layer are darker. The arrangement of atoms in the surface layer can be described by different planar tilings: a hexagon–rhombus tiling (full black lines), a Penrose tiling if each hexagon is divided into three thin rhombi (dashed red lines), or a triangle–rectangle tiling if all hexagons and rhombi are split as indicated by full red lines.

terminations, gG, pG, gP, and pP. Structural optimizations show that all possible surface terminations are stable; only modest changes of the interlayer distances and small but characteristic changes in the lateral interatomic distances are observed.

The determination of the stable termination of the nonstoichiometric 3-fold surfaces is a problem. The energetically most favorable cleavage plane may be determined using a simulated cleavage experiment,[27] predicting that the crystal cleaves between the MG and PG surfaces with an average surface energy of $\bar{\gamma}(\mathrm{MG} + \mathrm{PG}) = 1.16\ \mathrm{J/m^2}$, but cleavage between the pG and gP terminations with $\bar{\gamma}(\mathrm{pG} + \mathrm{gP}) = 1.19\ \mathrm{J/m^2}$ is also possible at a comparable energy. In both cases, a Ga-rich surface is found on one side and a Pd-rich one on the other side of the cleavage plane. The determination of the energies of individual surface terminations is difficult. Because of the polar character of the {111} surfaces, any slab cut perpendicular to the 3-fold direction exposes different surfaces. The calculated surface energies are correlated; the energy of any {111} surface depends on the energy of the $\{\overline{1}\overline{1}\overline{1}\}$ surface on the opposite site. Calculations for stoichiometric slabs produce the average surface energies of the terminations on both sides (including those determined by the simulated cleavage). Calculations for nonstoichiometric slabs must be performed in a grand canonical ensemble;[18,19] they can be used to derive the average Gibbs energies of different combinations of {111} and $\{\overline{1}\overline{1}\overline{1}\}$ surface terminations as a function of the chemical potential in the reactive atmosphere above the surfaces. The determination of the energies of individual surface terminations requires additional assumptions. For the {100} and {210} surfaces, the energy is approximately equal to the average of the surface energies of the pure metals. This suggests that in equilibrium a similar relation also holds also for the 3-fold surfaces, for example, that the ratio between the energies of the Ga-rich MG and the Pd-rich MP surfaces is equal to the ratio of the concentration weighted energies of the {111} surfaces of Ga and Pd.[27] An analogous assumption for any other pair of isostructural surfaces leads to the same result. The estimated values of the surface energies are compiled in Table 1; they correspond to surfaces stable under Ga-rich conditions.

Table 1. Estimated Surface Energies, γ ($\mathrm{J/m^2}$), of the Polar 3-fold Surfaces of GaPd with the B20 structure

surface A{111}	γ	surface A$\{\overline{1}\overline{1}\overline{1}\}$	γ
GP	0.86	GM	1.05
MG	0.90	PG	1.42
PM	2.06	MP	1.76
pG	1.05	gP	1.32
gG	0.74	pP	1.84

This means that the preferable bulk-terminated A{111} surface consists of a GP bilayer with three Ga atoms per surface cell in the upper and three Pd atoms in the lower part, whereas the A$\{\overline{1}\overline{1}\overline{1}\}$ surface is GM bilayer, with a sparse mixed Ga–Pd layer below the top Ga layer. Formally, a A{111}-GP surface decorated with Ga atoms in the hollows between the Ga_3 triplets (the gG termination) has an even lower surface energy, but it is difficult to see how this termination could be created by either cleavage (which would lead to the formation of the energetically very unfavorable pP termination on the other side of the cleavage plane) or crystal growth.[27]

Experimental studies of the 3-fold surfaces using X-ray and ultraviolet photoelectron spectroscopy, STM, and thermal desorption spectroscopy (TDS) of adsorbed CO have been presented by Rosenthal et al.[28] and Prinz et al.[29] The results indicate the formation of a smooth, essentially bulk-truncated surface with a (1×1) unit cell. For surfaces prepared at high temperature, a very sparsely populated surface with a single atom per surface cell has been reported, while a preparation at lower temperature leads to a denser population with three atoms per cell. TDS shows for the surface prepared at lower

dx.doi.org/10.1021/ar500043z | Acc. Chem. Res. 2014, 47, 3378–3384

temperature at least three desorption peaks at 120, 180, and 240 K and a saturation coverage of about five molecules per cell. Although these temperatures are dramatically reduced compared with those at which CO desorption from a pure Pd(111) surface is observed (about 450 K), a Pd-terminated surface was reported, based on the assumption that only Pd atoms are sufficiently reactive to bind CO.[28]

The DFT investigations lead to another conclusion. Figure 4 shows the atomic structure of the relaxed A{$\overline{111}$}-GM surface

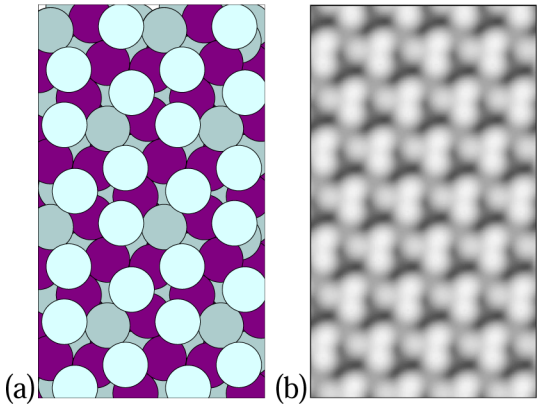

Figure 4. (a) Atomic structure (eight surface cells) and (b) simulated STM image (32 surface cells) of the A{$\overline{111}$}-GM surface of GaPd. Ga atoms are shown in light blue, Pd atoms in violet. Atoms in subsurface layers are darker.

and its simulated STM image. The bright contrast from the Ga triplet in the top plane is in excellent agreement with the experimental STM image of the surface prepared at lower temperature (cf. Figure 3 of Prinz et al.[29]), the clear separation of the bright spots in both images reflects the larger Ga−Ga distance (3.46 Å) compared with the Pd−Pd distance (2.92 Å) in the A{$\overline{111}$}-PG termination induced by the surface relaxation (in the bulk, the Ga−Ga and Pd−Pd distances are equal).

The analysis of the CO desorption also confirms that the A{111} surface is Ga-terminated. Figure 5a shows a top view of

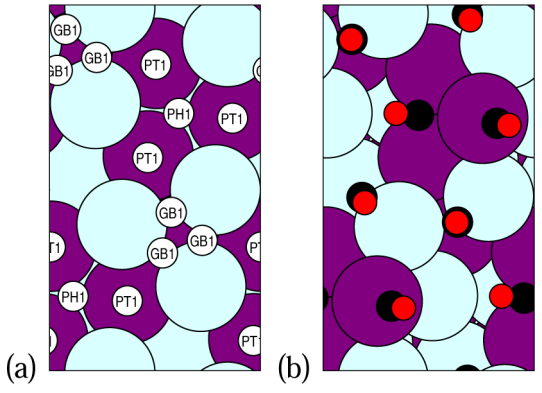

Figure 5. Atomic structure of the clean A{111}-GP surface and locally stable adsorption sites for CO molecules (a) and fully relaxed surface at maximum CO coverage (b). CO molecules are shown by the red and black dots. Note that upon CO adsorption both the Ga and the underlying Pd plane of the GP double layer undergo a considerable reconstruction.

the energetically favored A{111}-GP surface with the locally stable adsorption sites of CO molecules; Figure 5b shows the fully relaxed surface at maximum coverage of four CO molecules per surface cell. The calculated adsorption energies for isolated molecules vary between −60 kJ/mol in a hollow of the Pd triplet in the lower layer (site PH1) and −45 kJ/mol in a Ga−Ga bridge (GB1) site. The desorption energy for the most strongly bound CO molecule in the PH1 site is less than half the desorption energy of CO from a Pd(111) surface and well compatible with the highest peak in the observed TDS. The comparison of the surface densities of states with the ultraviolet photoelectron spectra[28] also confirms the predictions of Ga-terminated surfaces.

The investigation of the chemical properties of the 3-fold surfaces, however, demonstrates that the Ga-terminated surfaces are inactive as hydrogenation catalysts. To achieve the desired catalytic activity and selectivity, a mixed Ga/Pd occupation must be achieved.[30] The best catalytic performance is predicted for a A{$\overline{111}$}-gP surface. However, the calculations of the surface energies (cf. Table 1) show that this termination could be stabilized only under very special preparation conditions,[24,30] so in most cases the catalytic performance of GaPd stems from reactions in the {210} facets.

The energies for the possible low index also permit determination of the equilibrium shape of GaPd crystallites using a Wulff construction. The result is shown in Figure 6. The

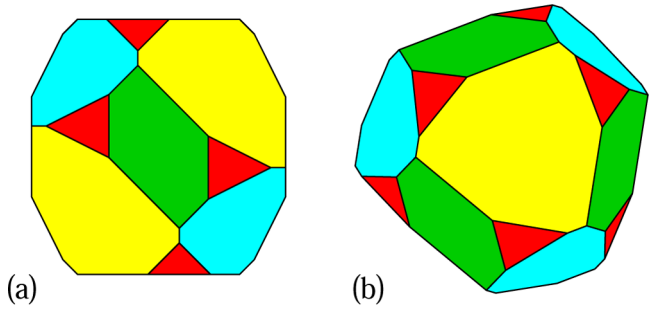

Figure 6. Equilibrium shape of a GaPd crystallite: (a) front view; (b) side view. Facets: {100}, green; {210}, red; A{111}, yellow; A{$\overline{111}$}, blue.

{210} facets occupy only a relatively small fraction of the crystallites grown under thermodynamic equilibrium conditions, but they dominate the catalytic performance.

■ ORTHORHOMBIC $Al_{13}Co_4$

The crystal structure of $Al_{13}Co_4$ is orthorhombic (Pearson symbol oP102, space group $Pmn2_1$, No. 31),[31] with 102 atoms per unit cell. The structure (see Figure 7) may be interpreted either in terms of an alternating stacking of flat (F) and puckered (P) (100) layers or in terms of large 23-atom clusters forming a pentagonal bipyramid (PB) consisting of a flat Al-centered decagonal ring in the central plane, capped by Co-centered Al pentagons on both sides. It has been shown that the strong covalent bonding along the central Co−Al−Co axis is important for the stability of the PBs.[32] The structure of $Al_{13}Co_4$ has received considerable attention as an approximant phase to decagonal Al−Co and decagonal Al−Ni−Co quasicrystals.[33,34] Very recently the interest in this compound has been renewed by the discovery that it represents an active and selective catalyst for the semihydrogenation of acetylene.[14,15]

$Al_{13}Co_4$ cleaves preferentially along (100) planes. From the interpretation of the crystal structure in terms of a stacking of flat and puckered layers one might expect that cleavage occurs

dx.doi.org/10.1021/ar500043z | Acc. Chem. Res. 2014, 47, 3378−3384

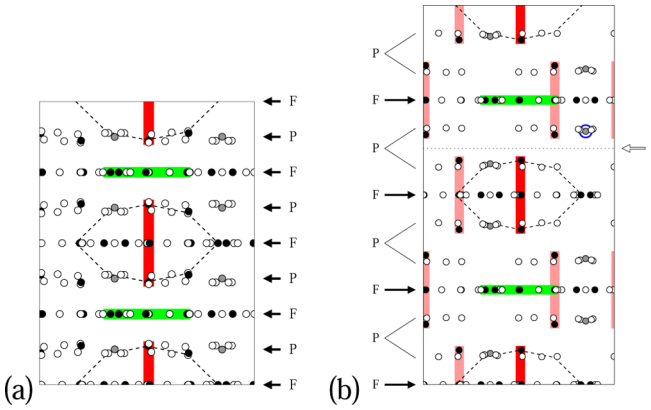

Figure 7. (a) Side view of the structure of $Al_{13}Co_4$: Al, open circles; Co, closed circles; the gray circles mark Al sites with a fractional occupancy. The PB clusters are marked explicitly by dashed lines. The PBs are stabilized by strong, partially covalent Co−Al−Co bonds marked by vertical red stripes. In the [100] direction, the PB clusters alternate with junction pentagons (marked in green) to form a "PB column". (b) Cleavage perpendicular to the [100] direction by splitting the layer such that the PBs remain intact. see text.

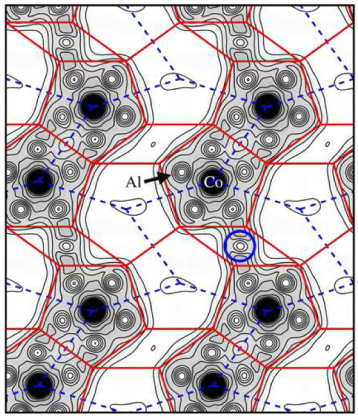

Figure 8. Contour plot of the electron density in the (100) surface of $Al_{13}Co_4$, calculated at the height of the incomplete P layer. Stripes of double $CoAl_5$ pentagons connected by thin rhombi are separated by a wide trough exposing the underlying F layer. The red full lines mark the pentagon−rhombus tiling describing the surface structure. Al atoms in the thin rhombi (blue circle) can easily desorb.

between adjacent flat (F) and puckered (P) layers. However, a simulated cleavage experiment[35] shows that the P layer splits into two complementary parts to preserve the integrity of very stable PB clusters [see Figure 7b]. The stable surface is terminated by an incomplete P layer consisting of the tips of the PB clusters and exposing in the interstices that part of the underlying F layer forming the connection between the PBs. Figure 8 shows the electron density in the incomplete P layer exposed at the surface. Double pentagons of Al atoms, centered by Co, are linked by thin rhombi decorated with a single Al atoms. These stripes are separated by wide troughs. The surface energy of this strongly corrugated, Al rich surface is surprisingly low, $\gamma = 1.19$ J/m^2; it is 0.1 J/m^2 lower than the average of the energies of the surfaces formed by cleaving between the F and P layers.

The as-cleaved surface undergoes only a modest relaxation, but individual atoms can be rather easily desorbed. The lowest desorption energy of only 0.4 eV has been calculated for the Al atom in the center of the thin rhombi, but it is remarkable that the energy for the desorption of the Co atom in the center of the pentagons is also lower than that of the surrounding Al atoms. The possible desorption of these atoms is important for the interpretation of the contrast in the STM images presented by Addou et al.[36] Figure 9 shows the simulated STM images. In part a, detailed images calculated for structures with and without an Al atom occupying the thin rhombus are shown; in part b, images of a larger surface area calculated for structures with (top) and without (bottom) the Co atom in the center of the pentagons are presented. Experimental images are shown in Figure 9c. Comparison of theory and experiment confirms that the surface indeed consists of the incomplete P layer predicted by the simulated cleavage experiment and that most of the Al atoms in the thin rhombi have been desorbed. The high-resolution image in part b shows weak dark spots in the center of some but not all $CoAl_5$ pentagons, similar to those in the calculated images.

GaPd AND $Al_{13}Co_4$ AS SELECTIVE SEMIHYDROGENATION CATALYSTS

$Al_{13}Co_4$ and GaPd have been identified as active and selective catalysts for the semihydrogenation of acetylene. The conditions to be met by a useful catalyst are the following: (i) The dissociative adsorption of hydrogen and a sufficient mobility of the hydrogen atoms on the surface must be favored. (ii) Acetylene and vinyl (produced by the first hydrogenation step) must be adsorbed strongly enough to be activated for further hydrogenation. (iii) Selectivity is achieved only if the desorption energy of ethylene is lower than the activation energy for further hydrogenation to ethyl. On the basis of the surface studies described above, an atomistic scenario for the catalytic reaction has been developed.[23,30,37] Dissociation of hydrogen is possible only if transition-metal atoms are present at the surface, but the atoms should be isolated because larger groups of transition-metal atoms act as traps for hydrogen atoms, limiting their mobility. On the surfaces of both

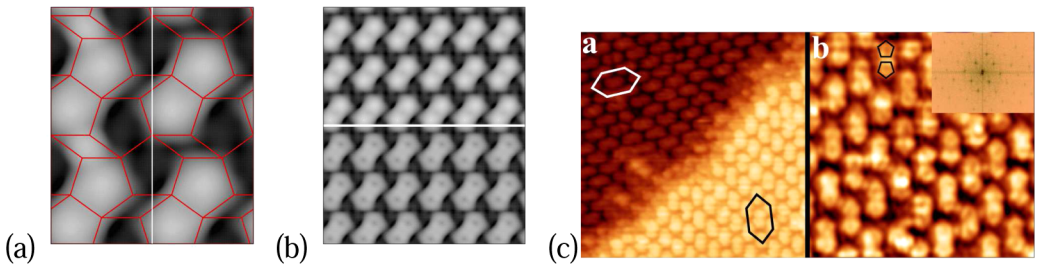

Figure 9. Simulated STM images of the (100) surface of $Al_{13}Co_4$: (a) Detailed images of two double pentagons calculated with (left) and without (right) an Al atom in the connecting thin rhombi. (b) Images of a larger surface area calculated with (top) and without (bottom) a Co atom in the center of the pentagons. (c) Experimental high-resolution STM image (after ref 36). See text.

dx.doi.org/10.1021/ar500043z | Acc. Chem. Res. 2014, 47, 3378−3384

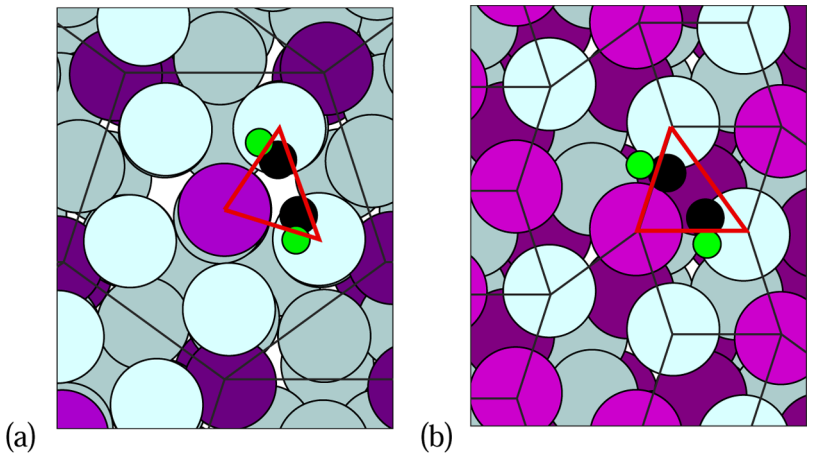

Figure 10. The catalytically active centers for the semihydrogenation of acetylene on the (pseudo)-5-fold (100) $Al_{13}Co_4$ (a) and {210} GaPd surfaces (b). The light blue circles represent Al or Ga atoms; the violet circles represent Co or Pd atoms, The red triangles mark the active reaction centers with a di-σ adsorbed acetylene molecule.

compounds, acetylene and the reaction intermediate vinyl are strongly di-σ bonded in a bridging configuration connecting two Ga(Al) atoms at the edge of a pentagon (see Figure 10). The modification of the local electronic structure on the Ga(Al) atoms caused by the covalent bonding to the transition-metal atoms is essential for the stabilization of the bridging adsorption configuration. After the second hydrogenation step ethylene is only weakly π-bonded to the central Co atom; the weak binding favoring desorption is responsible for the selectivity of the catalyst.

It is remarkable that although $Al_{13}Co_4$ and GaPd crystallize in such different structures, the catalytically active centers, a triangular arrangement of two simple (Al, Ga) and one transition metal (Co, Pd), are very similar. In both cases, the strong binding between the two constituents modifies the chemical reactivity of the simple-metal atoms. In contrast to the pure metal surfaces the atoms are reactive enough to form strong di-σ bonds and to activate the C−C single bonds of the reactant. The reaction product with C═C double bonds, however, can form only weaker bonds to the isolated transition-metal atom.

■ CONCLUSIONS

The insights offered by DFT studies of the surfaces of complex intermetallic compounds have been discussed at the example of B20-type GaPd (a lowest-order approximant to icosahedral quasicrystals) and of orthorhombic $Al_{13}Co_4$ (an approximant to decagonal quasicrystals). $Al_{13}Co_4$ has a complex structure with 102 atoms per cell built on pentagonal clusters stabilized by strong covalent Co−Al bonds. The simulated cleavage experiment is essential for determining the strongly corrugated surface that alone permits preservation of the integrity of the clusters. The crystal structure of GaPd with only eight atoms per unit cell is much simpler. While the determination of the {100} and {210} surfaces is easy and unambiguous, there are many possibilities, differing in structure and chemical composition, to terminate the polar {111} and $\{\overline{111}\}$ surfaces. Again simulated cleavage experiments, combined with calculations of the surface energies in the grand canonical ensemble, are very helpful. The comparison of simulated STM images with high-resolution experimental images permits examination of even rather fine details of the surface structures, such as the formation of vacant sites on the (100)-$Al_{13}Co_4$ surface and the slightly enhanced distances between Ga atoms in the stable A$\{\overline{111}\}$ surface of GaPd. However, because in the B20 structure Ga and Pd occupy isostructural sublattices and (almost) isostructural Ga- or Pd-terminated 3-fold surfaces are stabilized under different thermodynamic conditions, only the investigation of the chemical properties permits a unique characterization of the surface. The DFT calculation of the adsorption of CO molecules on the GaPd surfaces demonstrate that any interpretation of the experimental results should not be based on the known reactivities of the atoms in the pure metals, because the strong binding between unlike atoms in the intermetallic compound strongly modifies their chemical properties. The simple-metal atoms acquire a strongly enhanced reactivity, which is also important for understanding their surprising catalytic properties. The DFT studies also permit construction of atomistic scenarios for the catalytic reactions and identification of the active reaction centers, which are found to be surprisingly similar despite very different bulk crystal structures.

The discussions in this Account have concentrated on two characteristic examples, but the techniques used here have also been applied to other complex intermetallics. A recent example is the investigation of the (010) surface of the T-phase of $Al_3(Mn,Pd)$.[38]

■ AUTHOR INFORMATION

Corresponding Author

*E-mail: juergen.hafner@univie.ac.at.

Notes

The authors declare no competing financial interest.

Biographies

Jürgen Hafner received the doctoral degree in physics from Vienna University of Technology, Austria, in 1973. Afterwards he spent several years at the Max-Planck-Institute for Solid State Research in Stuttgart, Germany. In 1982, he was appointed Professor for Solid State Theory at Vienna University of Technology and in 1998 Professor for Solid State Physics at the University of Vienna. He was awarded the Krafft Medal by the Vienna University of Technology, the Ludwig-Boltzmann Prize by the Austrian Physical Society, and the Erwin-Schrödinger Prize by the Austrian Academy of Sciences. His current research focuses on the investigation of the structural, electronic, and chemical properties of solids, solid surfaces, and nanostructures using density-functional methods.

dx.doi.org/10.1021/ar500043z | Acc. Chem. Res. 2014, 47, 3378−3384

Marian Krajčí is a senior scientist in the Institute of Physics, Slovak Academy of Sciences. He is interested in the physics of metals, particularly surfaces of complex intermetallic compounds, their chemical reactivity, and their catalytic properties. Since 1991, he has collaborated with Prof. Hafner.

REFERENCES

(1) Diehl, R. D.; McGrath, R. Structural studies of alkali metal adsorption and coadsorption on metal surfaces. *Surf. Sci. Rep.* **1996**, *23*, 43−171.

(2) Woodruff, D. P. Solved and unsolved problems in surface structure determination. *Surf. Sci.* **2001**, *500*, 147−171.

(3) Belin-Ferré, E., Ed. *Basics of Thermodynamics and Phase Transitions in Complex Intermetallics*; World Scientific: Singapore, 2008.

(4) Suck, J. B., Schreiber, M., Häussler, P., Eds. *Quasicrystals*; Springer: Berlin, 2002.

(5) Thiel, P. A. An introduction to the surface science of quasicrystals. *Prog. Surf. Sci.* **2004**, *75*, 69−86.

(6) Ishii, Y., Fujiwara, T., Eds. *Quasicrystal Surfaces*; Elsevier: New York, 2008.

(7) Ledieu, J.; Munoz, A. W.; Parker, T. M.; McGrath, R.; Diehl, R. D.; Delaney, D. W.; Lograsso, T. A. Structural study of the fivefold surface of the $Al_{70}Pd_{21}Mn_9$ quasicrystal. *Surf. Sci.* **1999**, *433*−*435*, 666−671.

(8) Krajčí, M.; Hafner, J. Structure, stability, and electronic properties of the i-AlPdMn quasicrystalline surface. *Phys. Rev. B* **2005**, *71*, No. 054202.

(9) Krajčí, M.; Hafner, J.; Ledieu, J.; McGrath, R. Surface vacancies at the fivefold icosahedral Al-Pd-Mn quasicrystal surface: A comparison of *ab-initio* calculated and experimental STM images. *Phys. Rev. B* **2006**, *73*, No. 024202.

(10) Yuhara, J.; Klikovits, J.; Schmid, M.; Varga, P.; Yokoyama, Y.; Shishido, T.; Soda, K. Atomic structure of an Al-Co-Ni decagonal quasicrystalline surface. *Phys. Rev. B* **2004**, *70*, No. 024203.

(11) Krajčí, M.; Hafner, J.; Mihalkovič, M. *Ab-initio* study of the surface of a decagonal Al-Co-Ni quasicrystal. *Phys. Rev. B* **2006**, *73*, No. 134203.

(12) Osswald, J.; Giedigkeit, R.; Jentoft, R. E.; Armbrüster, M.; Girgsdies, F.; Kovnir, K.; Ressler, T.; Grin, Yu.; Schlögl, R. Palladium-gallium intermetallic compounds for the selective hydrogenation of acetylene: Part I: Preparation and structural investigation under reaction conditions. *J. Catal.* **2008**, *258*, 210−218. Osswald, J.; Kovnir, K.; Armbrüster, M.; Giedigkeit, R.; Jentoft, R. E.; Wild, U.; Grin, Yu.; Schlögl, R. Palladium-gallium intermetallic compounds for the selective hydrogenation of acetylene: Part II: Surface characterization and catalytic performance. *J. Catal.* **2008**, *258*, 219−227.

(13) Armbrüster, M.; Behrens, M.; Cinquini, M.; Föttinger, K.; Grin, Yu.; Haghofer, A.; Klötzer, B.; Knop-Gericke, A.; Lorenz, H.; Ota, A.; Penner, S.; Prinz, J.; Rameshan, Ch.; Révay, Z.; Rosenthal, D.; Rupprechter, G.; Sautet, P.; Schlögl, R.; Shao, L.; Szentmiklósi, L.; Teschner, D.; Torres, D.; Wagner, R.; Widmer, R.; Wowsnick, G. How to control the selectivity of palladium-based catalysts in hydrogenation reactions. *ChemCatChem* **2012**, *4*, 1048−1063.

(14) Armbrüster, M., Kovnir, K., Grin, Yu., Schlögl, R., Gille, P., Heggen, M., Feuerbacher, M., Ordered cobalt-aluminum and iron-aluminum intermetallic compounds as hydrogenation catalysts, European Patent Application EP09157875.7, 2009.

(15) Armbrüster, M.; Kovnir, K.; Friedrich, M.; Teschner, D.; Wowsnick, G.; Hahne, M.; Gille, P.; Szentmiklósi, L.; Feuerbacher, M.; Heggen, M.; Girgsdies, F.; Rosenthal, D.; Schlögl, R.; Grin, Yu. $Al_{13}Fe_4$ as a low-cost alternative for palladium in heterogeneous hydrogenation. *Nat. Mater.* **2012**, *11*, 690−693.

(16) Kresse, G.; Joubert, D. From ultrasoft pseudopotentials to the projector-augmented wave method. *Phys. Rev. B* **1999**, *59*, 1758−1775.

(17) Hafner, J. Ab-initio materials simulation using VASP: Density-functional theory and beyond. *J. Comput. Chem.* **2008**, *29*, 2044−2078.

(18) Finnis, M. W. Accessing the excess: A atomistic approach to excesses at planar defects and dislocations in ordered compounds. *Phys. Stat. Solidi A* **1998**, *166*, 397−416.

(19) Reuter, K.; Scheffler, M. Composition, structure and stability of $RuO_2(110)$ as a function of oxygen pressure. *Phys. Rev. B* **2001**, *65*, No. 035406.

(20) Tersoff, J.; Hamann, D. R. Theory of the scanning tunneling microscope. *Phys. Rev. B* **1985**, *31*, 805−813.

(21) Gille, G.; Ziemer, T.; Schmidt, M.; Kovnir, K.; Burkhardt, U.; Armbrüster, M. Growth of large PdGa single crystals from the melt. *Intermetallics* **2010**, *18*, 1663−1668.

(22) Krajčí, M.; Hafner, J. Topologically induced semiconductivity in icosahedral Al-Pd-Re and its approximants. *Phys. Rev. B* **2007**, *75*, No. 024116.

(23) Krajčí, M.; Hafner, J. The (210) surface of the intermetallic compound GaPd as a selective hydrogenation catalyst: A DFT study. *J. Catal.* **2012**, *295*, 70−80.

(24) Krajčí, M.; Hafner, J. Structure and chemical reactivity of the polar three-fold surfaces of GaPd: A density-functional study. *J. Chem. Phys.* **2013**, *138*, No. 124703.

(25) Krajčí, M.; Hafner, J. Magnetism and chemical ordering in icosahedral Al-Pd-Mn quasicrystals. *Phys. Rev. B* **2008**, *78*, No. 224207.

(26) Krajčí, M.; Hafner, J. Theory of quasicrystal surfaces: Probing the reactivity by atomic and molecular adsorption. *Surf. Sci.* **2008**, *602*, 182−197.

(27) Krajčí, M.; Hafner, J. Surfaces of intermetallic compounds: An ab-initio DFT study for B20-type AlPd. *Phys. Rev. B* **2013**, *67*, No. 035436.

(28) Rosenthal, D.; Widmer, R.; Wagner, R.; Gille, P.; Armbrüster, M.; Grin, Y.; Schlögl, R.; Grönig, O. Surface investigation of intermetallic PdGa{111}. *Langmuir* **2012**, *28*, 6848−6856.

(29) Prinz, J.; Gaspari, R.; Pignedoli, C. A.; Vogt, J.; Gille, P.; Armbrüster, M.; Brune, H.; Gröning, O.; Passerone, D.; Widmer, R. Isolated Pd sites on intermetallic PdGa(111) and PdGa(−1−1-1) model catalyst surfaces. *Angew. Chem., Int. Ed.* **2012**, *51*, 9339−9343.

(30) Krajčí, M.; Hafner, J. Selective semi-hydrogenation of acetylene: Atomistic scenario for reactions on the polar threefold surfaces of GaPd. *J. Catal.* **2014**, *312*, 232−248.

(31) Grin, J.; Burkhardt, U.; Ellner, M.; Peters, K. Crystal structure of orthorhombic Co_4Al_{13}. *J. Alloys Compd.* **1994**, *206*, 243−247.

(32) Jeglič, P.; Vrtnik, S.; Bobnar, M.; Kljanšek, M.; Bauer, B.; Gille, P.; Grin, Y.; Haarmann, F.; Dolinšek, J. M-Al-M groups trapped in cages of $Al_{13}M_4$ (M = Co, Fe, Ni, Ru) intermetallic phases as seen via NMR. *Phys. Rev. B* **2010**, *82*, No. 104201.

(33) Henley, C. L. Current models of decagonal atomic structure. *J. Non-Cryst. Solids* **1993**, *153*−*154*, 172−176.

(34) Krajčí, M.; Hafner, J.; Mihalkovič, M. Atomic and electronic structure of decagonal Al-Ni-Co alloys and approximant phases. *Phys. Rev. B* **2000**, *62*, 243−255.

(35) Krajčí, M.; Hafner, J. Surface structure of complex intermetallic compounds: An ab-initio DFT study for the (100) surface of o-$Al_{13}Co_4$. *Phys. Rev. B* **2011**, *84*, No. 115410.

(36) Addou, R.; Gaudry, E.; Deniozou, Th.; Heggen, M.; Feuerbacher, M.; Gille, P.; Grin, Yu.; Widmer, R.; Gröning, O.; Fournée, V.; Dubois, J.-M.; Ledieu, J. Structure investigation of the (100) surface of orthorhombic $Al_{13}Co_4$. *Phys. Rev. B* **2009**, *80*, No. 014203.

(37) Krajčí, M.; Hafner, J. Complex intermetallic compounds as selective hydrogenation catalysts: A case study for the (100) surface of $Al_{13}Co_4$. *J. Catal.* **2011**, *278*, 200−207.

(38) Deniozou, Th.; Addou, R.; Shukla, A. K.; Heggen, M.; Feuerbacher, M.; Krajčí, M.; Hafner, J.; Widmer, R.; Gröning, O.; Fournée, V.; Dubois, J.-M.; Ledieu, J. *Phys. Rev. B* **2010**, *81*, No. 125418.